

PPS021-01

Room:101

Time:May 23 08:30-08:45

Development of Laser Ionization Mass Nanoscope: LIMAS

Shingo Ebata^{1*}, Morio Ishihara¹, Kiichiro Uchino², Satoru Itose³, Miyuki Matsuya³, Masato Kudo³, Hisayoshi Yurimoto⁴

¹Osaka University, ²Kyushu University, ³JEOL Ltd., ⁴Hokkaido University

Many sample-return missions are planned in the world (e.g. JAXA Hayabusa, NASA Stardust). Samples are collected on asteroids or comets, returned to the Earth, and then analyzed in laboratories. However, a very small amount of samples can be brought back because of the limitations on the space probes. Thus ultra-high sensitivity, lateral resolution, and resolving power are required for the mass spectrometer.

Here we have been developing a novel TOF-SIMS system; prototype in Osaka Univ. and new-type in JEOL Ltd.. This instrument consists of a FIB system with a liquid metal Ga ion source, a femto-second laser for post-ionization and a multi-turn TOF-MS 'MULTUM II'.

Firstly, in order to evaluate the performance of quantitative analysis, several alloys and standard glass JB-2 were analyzed using the prototype system. Alloys used for this evaluation were Constantan, Cupronickel, Brass, Inconel-625, SUS301, SUS310, and SUS321 (the Nilako corp., Japan).

Secondly, in order to evaluate the postionization efficiency and mass resolving power using the new-type system 'LIMAS', non-postionization (SIMS) and postionization mode were compared. Samples used for this evaluation were Al for SIMS mode and Ag substrate for postionization mode, respectively.

Chemical compositions of constantan, cupronickel, and brass were corresponded approximately to reference values in the error ranges. Chemical compositions of SUS301, SUS310 and SUS321 were slightly higher intensity of Cr and slightly lower of Ni than those of reference values. These results show this instrument was useful for quantitative analyses. On the other hand, Chemical compositions of inconel-625 was very higher of Cr than those of reference value.

The postionization efficiency and mass resolution using the new-type system 'LIMAS' were evaluated. By using post-ionization, the secondary ion signals of Ag were increased ~6000 times compared with the conventional TOF-SIMS experiments. This result shows that the nonresonant multiphoton post-ionization experiments have superior sensitivity. Compared to the prototype experiments, the secondary ion signals of Ag were increased ~3 times, because the pulse width of a femto-second laser was improved from 120 fs to 40 fs.

The mass resolution was achieved to ~12000 by SIMS mode (flight length: ~70 m at 50 cycles) and ~15000 by LIMAS mode (flight length: ~35 m at 25 cycles). These results show this instrument was useful for isotope analyses.

These results indicated that this instrument would be very effective for ultrahigh sensitivity analysis of nano-size particles such as Hayabusa mission return samples.

Keywords: Hayabusa, SNMS, Focused ion beam, Femto second laser, Multi-turn mass spectrometry

PPS021-02

Room:101

Time:May 23 08:45-09:00

Microspectroscopic analysis of iron meteorite using photoelectron emission microscopy (PEEM)

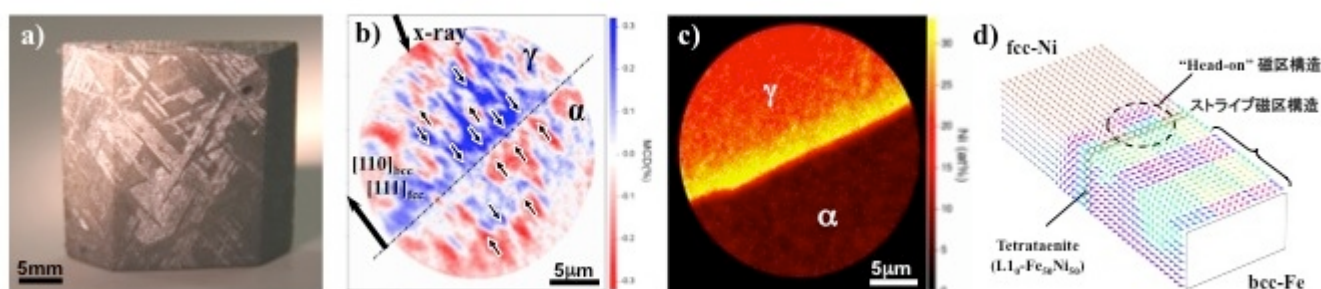
Masato Kotsugi^{1*}

¹SPring-8/JASRI

The magnetic properties of iron meteorites greatly differ from those of iron-nickel alloys found on Earth, the reason for which has long been veiled in mystery. The scientists of this research team approached this mystery of the magnetic properties of iron meteorites by accurately evaluating their physical properties from the viewpoint of materials science and, at the same time, considering that such accurate evaluation will be effective for the exploration of other magnetic materials.

They directly observed iron meteorites at the nanometer level using a photoemission electron microscope (PEEM) at SPring-8, and discovered a new magnetic domain structure, which has never been found in conventional iron-nickel alloys. (PEEM is a cutting-edge microscope that came under the spotlight because of its use in the research awarded the 2007 Nobel Prize in Chemistry.) By comparing the magnetic domain structure obtained in the experiments with that obtained by simulation, it was clarified that the magnetic domain structure originates from tetrataenite, an iron-nickel phase unique to iron meteorites.

This tetrataenite phase, originating from the universe, does not contain rare metals and exhibits excellent functionalities; therefore, it is expected to lead to the achievement of high density and power saving as well as resource saving in next-generation magnetic devices. Currently, the artificial creation of tetrataenite and the evaluation of its physical properties are ongoing, aiming towards its application to such devices, which are expected to have a productive ripple effect on future green nanotechnology.



Keywords: iron meteorite, synchrotron radiation, photoelectron emission microscopy, microscopy, magnetic structure, paleomagnetism

PPS021-03

Room:101

Time:May 23 09:00-09:15

Nondestructive characterization of a single micron-sized primitive-grain realized by magnetic ejection in microgravity

Keiji Hisayoshi^{1*}, Chiaki Uyeda¹

¹Graduate School of Science, Osaka Unives

A new principle is proposed for the characterization of a single grain sample. This principle is based on a translation induced by a magnetic field-gradient force that was recently found on diamagnetic solids [1][2]. A single mm-sized sample was released in an area field gradient that was located in microgravity condition. According to a motional equation of translation, acceleration of sample was uniquely determined by intrinsic magnetic susceptibility of the material in a given field distribution. Hence susceptibility of the sample was detected by observing field-induced motion of the sample. Since a published value of diamagnetic susceptibility exist for a solid material, the identification of material is possible by comparing the measured susceptibility data with the compiled list of published values. Conventional magnetization measurements in normal gravity are generally prevented by background signal of sample holder when size of sample is smaller than 1 mm in diameter. The mass measurement of the sample is difficult below the level of 100 micro grams. In contrast, it is expected that the proposed method can measure susceptibility of a single grain with limitlessly small size, provided that the observation of the grain motion is possible; material identification of the small becomes possible as well.

The conventional facilities of microgravity are not suitable for a routine analysis such as the present measurement of susceptibility. This is because the facility system requires a long machine time; its running cost is considerably high. Therefore, a compact microgravity system, which can be introduced in an ordinary laboratory, was newly developed. The length of the drop shaft is 1.5m, and the duration of microgravity time is 0.62 second. The experimental apparatus was set inside a rectangle box which had a size of 30cmx30cmx20cm. The vacuum chamber equipped with an electric actuator, sample releasing signal reception device, the sample holder controller, the magnet, the battery, and the high-vision video camera are installed in the box. The sample is released in the field-gradient produced by a by a magnetic circuit composed by a NdFeB permanent magnet. Maximum field intensity of the circuit was 0.7 T. The box was attached to the sealing of the laboratory room by an electromagnetic lock system. The free fall of the box started shortly after the power supply of the lock was shut down. Image of sample translation was recorded by the HV camera.

In the present work, translation was observed for small particle as small as 50 micron for graphite and the diamond. The spatial and time resolution of the present system can be improved by introducing a macro-lens, and by recording the image by a high-speed photography. The above mentioned improvements is expected to identify the sample of about 20 micron. If a single small particle can be identified nondestructively, the possibility of analyzing individual particle that compose primitive meteorite is expected to increase drastically. The observed magnetic susceptibility is in the range of -5×10^{-6} emu/g from -2×10^{-7} . It is expected that the diamagnetic susceptibility of the organic matter contained in the meteorites distribute in this range.

[1] K. Hisayoshi, S. Kanou and C. Uyeda: J.Phys.:Conf.Ser., 156 (2009) 012021

[2] C. Uyeda, K. Hisayoshi and S. Kanou: Jpn. Phys. Soc. Jpn. 79 (2010) 064709

Keywords: diamagnetic susceptibility measurement, nondestructive characterization, microgravity, magnetic ejection, field gradient force

PPS021-04

Room:101

Time:May 23 09:15-09:30

Oxygen isotopic compositions of melilite in Fluffy Type A CAI from Efremovka meteorite

Noriyuki Kawasaki^{1*}, Naoya Sakamoto², Hisayoshi Yurimoto³

¹Natural History Sci., Hokudai, ²CRIS, Hokudai, ³Natural History Sci., Hokudai

Calcium-Aluminum-rich inclusion (CAI) is the oldest rock in the solar system and preserves a record of events in the early solar system. Reversely zoned crystals of melilite have been found in Fluffy Type A CAIs, and have been condensed directly as solids from a hot nebular gas in the early solar system (MacPherson and Grossman 1984). In this study, oxygen isotopic compositions and chemical compositions of melilite crystals in a Fluffy Type A CAI of Efremovka CV3 chondrite has been described. A polished thin section of the CAI was used. Petrographic studies and the chemical compositions have been measured by a field emission type secondary electron microscope equipped with an energy dispersive spectrometer (FE-SEM-EDS, JEOL JSM-7000F; Oxford INCA Energy). Crystal orientations of the CAI melilite have been determined by an electron back scattered diffraction system (EBSD, HKL Channel 5) equipped with the SEM in order to determine crystal boundaries of the melilite grains. Oxygen isotopic compositions have been measured by secondary mass spectrometry (SIMS, Cameca ims-1270).

The CAI is 10 x 3 mm in size with fluffy shape. The CAI has core-mantle structure. The core part contains of large amounts of spinel which are poikilitically enclosed by anorthite, melilite and Al-Ti-rich diopside. The mantle part mainly consists of melilite, Al-Ti-rich diopside. The abundance of spinel is smaller than in the core part. A Wark-Lovering Rim (WL-Rim) surrounds the mantle. Typical size of mantle melilite crystal is 15-25 micrometers. From the distribution of chemical compositions and oxygen isotopic compositions of melilite in the mantle are classified into two distinct regions.

The first region in the mantle, domein-1, shows that melilite crystals positioned shallower than ~200 micrometers in depth from the WL-Rim have grown as reverse zoning. Compositions of the crystal center and grain boundary are $\delta^{18}\text{O} \sim +25$ and $\delta^{18}\text{O} \sim +5$, respectively. The oxygen isotopic compositions of single crystals are distributed homogeneously within the analytical error. However, oxygen isotopic compositions are systematically changed among crystals. The melilite crystals positioned near WL-rim are more ^{16}O -rich ($\text{DELTA-17O} = -19$ permil) while the melilite crystals near the CAI core are ^{16}O -poor ($\text{DELTA-17O} = -4$ permil). The oxygen isotopic compositions change continuously from rim to core of the CAI.

The second region in the mantle, domein-2, melilite crystals positioned shallower than ~40 micrometers in depth from the WL-Rim have grown as reverse zoning. Compositions of the crystal are $\delta^{18}\text{O} \sim +25$ in the center and $\delta^{18}\text{O} \sim +8$ at the grain boundary. While the melilite crystals of domein-2 positioned deeper than the ~40 micrometers have grown initially as reverse zoning and then grown as normal zoning, i. e., oscillated. The compositions are $\delta^{18}\text{O} \sim +30$ in the center, $\delta^{18}\text{O} \sim +45$ in the intermediate, and $\delta^{18}\text{O} \sim +55$ at the grain boundary. Typical width of the normal zoning part is 2-5 micron. Oxygen isotopic composition of melilite crystals existed in the domein-2 are homogeneously distributed, $\text{DELTA-17O} = -3$, despite of complex growth patterns.

The oxygen isotopic heterogeneity observed in the domein-1 suggests that oxygen isotopic ratios of nebular gas surrounding the melilite growing did not changed during the growth of each melilite crystal, while gradually changed from ^{16}O -poor to ^{16}O -rich during the total duration of melilite formation of domein-1. In this nebular condition, the melilite was directly condensed from the nebular gas and accumulated together. The oxygen isotopic compositions observed in domein-2 suggest that the melilite seems to be directly condensed from ^{16}O -poor nebular gas and accumulated together. Then the domein-1 and domein-2 were accreted together. After that, moderate heating of the CAI occurred. Grain boundaries of melilite of domein-2 were partially molten because of the high $\delta^{18}\text{O}$ compositions. The normally zoned melilite was overgrown on relicts of melilite during cooling.

Keywords: CAI, melilite, oxygen isotope, solid solution, chondrite

PPS021-05

Room:101

Time:May 23 09:30-09:45

Oxygen isotope zoning in reversely zoned melilite in Fluffy Type A CAI from Vigarano meteorite

Juri Katayama^{1*}, Shoichi Itoh¹, Hisayoshi Yurimoto¹

¹Natural History Sci., Hokudai

The oxygen isotopic variations of each mineral in the Ca-Al-rich inclusions (CAI) are due to mass-independent fractionation and plot along a CCAM line with slope of ~ 1 (Clayton et al., 1973). These variations indicate that CAI minerals were not derived entirely from a chemically homogeneous, well-mixed reservoir, but from mixing of ^{16}O -rich and ^{16}O -poor reservoir (e.g., Clayton., 1993). In previous in-situ oxygen isotope analyses, the oxygen isotope distribution of each CAI mineral go along a CCAM line results from the oxygen isotope exchange among ^{16}O -poor gas reservoirs and ^{16}O -rich CAI melt occurred by multiple partial melting process in the CAI forming region (Yurimoto et al., 1998). In addition, the oxygen isotopic compositions of each mineral in fine-grained CAI condensed from gas are enriched in ^{16}O (e.g., Krot et al., 2002). However, the relationship among two reservoirs in the CAI forming region is not clear.

Fluffy Type A CAI (FTA) condensed as solids from the hot solar nebular gas, based on their irregular shaped and the existence of reversely-zoned melilite crystals (MacPherson and Grossman, 1984). Therefore the intra-grain distribution of oxygen isotopes in FTA is critical to discussion of the oxygen isotopic composition of nebular gas, because these inclusions are believed to be direct condensates from the nebula (Yurimoto et al., 2008). In this study, we report the in-situ oxygen isotope distribution corresponding to the reversely-zoned melilite crystal in order to estimate the relationship between ^{16}O -rich and ^{16}O -poor gas reservoirs in the CAI forming region.

X-ray mapping with ~ 1 micron spatial resolution using FE-SEM-EDS determined compositional zoning of melilite crystals. Grain boundary was determined by orientation mapping using FE-SEM-EBSD. A line profile of oxygen isotope distribution of melilite crystal was obtained across the reversely zoning using Cameca ims-1270 SIMS with 3-5 micron spot.

Most melilite crystals in V2-01 FTA show the reversely zoned melilite using the estimation of grain boundary of melilite crystal with the effect of deformation and compaction in the parent body. The intra-grain distribution of oxygen isotopes in melilite crystals indicates that some melilite crystals show the oxygen isotope zoning with ~ 30 permil whereas shows no oxygen isotopic zoning. Two melilite single crystals (Grain 8 and 21) were estimated oxygen isotopic zoning with line profile correlated with reverse zoning. In the reverse zoning of Grain 8, ak content gradually change with the range of ~ 90 micron from core ($\sim \text{ak}_{14}$) to rim ($\sim \text{ak}_5$). The oxygen isotopic ratio changes with the range of ~ 40 micron from ^{16}O -poor ($\delta^{18}\text{O}_{\text{SMOW}} = -20$ permil, $\sim \text{ak}_8$) to ^{16}O -rich ($\delta^{18}\text{O}_{\text{SMOW}} = -30$ permil, $\sim \text{ak}_5$). In the reverse zoning of Grain 21, ak content gradually change with the range of ~ 65 micron from core ($\sim \text{ak}_{23}$) to rim ($\sim \text{ak}_2$). The oxygen isotopic ratio changes with the range of ~ 15 micron from ^{16}O -poor ($\delta^{18}\text{O}_{\text{SMOW}} = -15$ permil, $\sim \text{ak}_4$) to ^{16}O -rich ($\delta^{18}\text{O}_{\text{SMOW}} = -40$ permil, $\sim \text{ak}_2$). This means that the line profile shows, correlated with a gradual decrease in akermanite content, a change of oxygen isotopic ratios from ^{16}O -poor to ^{16}O -rich in the range of $15 \sim 40$ micron.

These results indicates that oxygen isotopic compositions of the gas reservoirs changed from ^{16}O -poor to ^{16}O -rich during crystallization of single melilite crystals. As results, there are gas reservoirs with oxygen isotope fluctuation changes from ^{16}O -poor to ^{16}O -rich in the CAI forming region.

A new constraint for chondrule formation: condition for rapid crystal growth along droplet surface

Hitoshi Miura^{1*}, Etsuro Yokoyama², Ken Nagashima³, Katsuo Tsukamoto¹

¹Tohoku University, ²Gakushuin University, ³Osaka University

Barred-olivine (BO) chondrules are characterized by parallel set(s) of olivine bar crystals, which are platy in three-dimension [1,2]. A BO chondrule usually has an olivine crystal that covers the chondrule surface (rim). The olivine rim has the same crystallographic orientation as the inner olivine platelets. Tsukamoto et al. succeeded to reproduce the rim structure from a forsterite melt droplet in their container-less crystallization experiment using aero-acoustic levitation technique [3]. They found that the droplet cooled very rapidly at a rate of $R_{cool} \sim 100 - 1000 \text{ K s}^{-1}$, and then crystallized within a very short period of time less than $\sim 1 \text{ s}$ at a large supercooling of $DT \sim 600 \text{ K}$. On the other hand, Tsuchiyama et al. also succeeded in reproducing the rim structure by evaporation in vacuum [4]. The cooling rate was $R_{cool} = 1000 \text{ K hr}^{-1}$, which is much slower than [3] by about three orders of magnitudes. Tsuchiyama et al. considered that the rim was formed by the rapid crystal growth along the droplet surface, which should become cooler than the interior by the latent heat of the evaporation. However, their hypothesis has not been verified yet.

To understand the formation mechanism of the rim structure, the crystal growth pattern inside the chondrule melt droplet should be investigated. We carried out numerical simulations of crystallization of a highly-supercooled melt droplet by using a phase-field method [5]. We considered the situation that a tiny crystal seeded at the droplet surface triggers crystallization of the droplet. We found that the rapid crystal growth along the droplet surface occurs when the cooling rate is considerably large. However, they did not investigate for a wide range of the supercooling of the droplet.

In this study, we investigated the condition of the rapid crystal growth along the droplet surface by using the phase-field method. We considered the cases that the seeding occurs when the surface of the droplet is supercooled by $DT_s = 200, 300, 400, 500,$ and 600 K . The surface of the droplet cools at a constant heat flux; $q_s = 5 \times 10^8, 1 \times 10^9, 2 \times 10^9, 5 \times 10^9,$ and $1 \times 10^{10} \text{ erg cm}^{-2} \text{ s}^{-1}$ for each DT_s . Because of the surface cooling, the droplet surface becomes cooler than the center by $dT_{c-s} \sim 30 - 600 \text{ K}$ for the droplet radius $r_d = 250 \text{ um}$ ($\text{um} = \text{micro-meter}$). We found that the rapid crystal growth along the droplet surface occurred when $dT_{c-s} \sim 100 - 200 \text{ K}$ or larger. The minimum value of dT_{c-s} for the rapid crystal growth along the droplet surface increases as DT_s increases. To derive the minimum value of dT_{c-s} analytically, we compared crystal growth timescales via two different routes inside the droplet; along the droplet surface, and across the droplet center. We found that the growth timescale along the surface becomes shorter than that across the center when $a = dT_{c-s} / DT_s > \sim 0.2$, which condition is rewritten by $R_{cool} > \sim 2000 (DT_s / 300 \text{ K}) (r_d / 250 \text{ um})^{-2} \text{ K s}^{-1}$. This condition is applicable for limited cases that satisfy the following two conditions; (a) crystal growth timescale is much shorter than a cooling timescale of the droplet, and (b) the supercooled droplet is a single component system, namely, the chemical composition of crystal is the same as the parent liquid. If the crystal growth kinetics depends on the growth direction, which usually comes from its crystal structure, we need small modification to the critical values of a and R_{cool} [5]. The new constraint for the rapid crystal growth along the droplet surface is applicable for limited cases, however, this is the first step to understand the formation mechanism of BO chondrule solidification texture.

Reference: [1] Tsuchiyama et al., *J. Geography*, **109**, 845-858, 2000 (in Japanese). [2] Noguchi, *Antarctic Meteorite Research*, **15**, 59-77, 2002. [3] Tsukamoto et al., *Antarct. Meteorites*, **24**, 179-181, 1999. [4] Tsuchiyama et al., *Geochim. Cosmochim. Acta*, **68**, 653-672, 2004. [5] Miura et al., *J. Appl. Phys.*, **108**, 114912, 2010.

Keywords: chondrule, barred olivine, formation condition, crystal growth

Japan Geoscience Union Meeting 2011

(May 22-27 2011 at Makuhari, Chiba, Japan)

©2011. Japan Geoscience Union. All Rights Reserved.



PPS021-07

Room:101

Time:May 23 10:00-10:15

Classification of micrometeorites bearing coarse-grained relict minerals

Naoya Imae^{1*}, Susan Taylor², Naoyoshi Iwata³

¹National Institute of Polar Research, ²U.S. ACRREL, ³Yamagata University

Micrometeorites bearing relict minerals survived the atmospheric entry heating have been studied.

Keywords: micrometeorites, classification, chondrites, meteorites

PPS021-08

Room:101

Time:May 23 10:45-11:00

REE pattern and oxygen isotopes in a unique granular-olivine inclusion from the Murchison (CM2) meteorite

Mutsuo Inoue^{1*}, Itoh Shoichi², Kimura Makoto³, Yurimoto Hisayoshi², Noboru Nakamura⁴

¹Kanazawa University, ²Hokkaido University, ³Ibaraki University, ⁴NASA Johnson Space Center

A homogeneous granular-olivine (Fa38.5) inclusion (MI-GO) carrying minor merrillite and nepheline was collected from the Murchison (CM2) meteorite, and analyzed for rare earth (REE; La, Ce, Nd, Sm, Eu, Gd, Dy, Er, Yb, and Lu) and other trace elements (K, Rb, Sr, and Ba) by isotope dilution, together with petrographical observation. The inclusion shows no evidence for aqueous alteration petrologically and chemically but indicates conspicuous REE fractionations; light-REE (L-REE) enriched, smoothly heavy-REE depleted pattern (La, $6.1 * CI$; CI-norm. La/Lu ratio = 3.0) with a large negative Eu anomaly (~70% negative), high FeO content (30%) and fractionated alkali abundances (CI-norm. K/Rb = 2.2). The observed bulk REE pattern is substantially different from those of aqueously altered CM chondrules and also from any kind of chondrules and CAIs from carbonaceous and unequilibrated ordinary chondrites (UOCs), but relatively similar to those of some kind of achondrite and of lunar KREEP basalts. The unique REE features, being similar to so-called geochemical fractionation, can not be explained as being due to nebular fractionation nor aqueous alteration processes, but are well understood as having been resulted from equilibrium partitioning of solid/melt and/or solid/solid interaction in the planetesimal setting. The holocrystalline texture, the occurrence of crystalline nepheline and homogeneous FeO-rich olivine suggest that MI-GO experienced melting and slow cooling or metamorphism and was then incooperated into the Murchison parent body during the early regolith-forming processes. To clarify the origin and precursor materials of MI-GO, we measured oxygen isotopic compositions in olivine groundmass using the Cameca ims-1270 ion microprobes. Combining the result of oxygen isotopic compositions, we discuss the formation process of MI-GO and the early planetary differentiation in the parent planetesimal.

PPS021-09

Room:101

Time:May 23 11:00-11:15

Diverse formation history recorded in two reduced-type carbonaceous chondrites RBT04143 and QUE97186

Hatsumi Ishida^{1*}, Tomoki Nakamura¹, Hitoshi Miura¹, Yuki Kakazu²

¹Tohoku University, ²Kyushu University

We have carried out mineralogical and oxygen isotopic analysis on two reduced-type carbonaceous chondrites, RBT04143, QUE97186, in order to estimate their formation and evolution processes.

According to polarized optical microscope observation, RBT04143 has porous matrix and rounded chondrules. On the other hand, the matrix of QUE97186 is highly compacted with porosity much lower than RBT04143 and chondrules are flattened to high aspect ratios and show a preferred orientation. This texture strongly suggests that the meteorite has experienced shock impact on the meteorite parent body. Olivine and pyroxene in QUE97186 chondrules show undulatory extinctions and planar deformation fractures. This result indicates that the meteorite experienced shock pressure around 20GPa based on the comparison to the results of previous shock recovery experiments (Nakamura et al., 2001) and polarizing microscope analysis (Stoffler et al., 1991).

To estimate the intensity of thermal metamorphism, we measured Fa# in fine-grained matrix olivine using FE-EPMA. As a result, Fa# in QUE97186 ranges from 40 to 60 but Fa# in RBT04143 shows a wider range (0 to 90). The wide Fa# variation in RBT04143 indicates that small silicate particles in the solar nebula have an extreme wide range of Fe/Mg ratios and RBT04143 has undergone least degrees of aqueous alteration and thermal metamorphism. Meanwhile, the narrow range of Fa# in QUE97186 is likely due to shock heating.

That the fine-grained matrix olivine escaped thermal metamorphism indicates CAI and chondrule in RBT04143 preserves the records of processes taken place in the early solar nebula. Oxygen isotope ratios of a type-B CAI and a type-II chondrule were measured by a secondary ion mass spectrometer (SIMS CAMECA ims-6f). The type-B CAI consists of melilite, fassaite, and diopside and these crystals locate from inner core to outer rim. The inner melilite shows ¹⁶O-poor composition, but outer diopside shows ¹⁶O-rich, suggesting that oxygen isotope exchange occurred between a nebula gas and the CAI at a temperature below melting point at which diffusion rates varies greatly between these minerals.

There are some relict Mg-rich olivine grains in the Type-II chondrule. Oxygen isotope ratios of Fe-rich olivine are homogeneous but the relict Mg-rich olivine is enriched in ¹⁶O. This indicates that the Mg-rich olivine preserves isotope composition of precursor grains, but other phases were melted and exchange oxygen with a nebula gas during heating.

Matrix in QUE97186 preserves evidence of impact. Some sulfides in the matrix are partially molten due to shock heating and the matrix was heated to temperature over 1170C. During cooling from this temperature, Fa# of fine-grained matrix olivine became homogenized. So as to estimate the cooling rate, simulation of changes of Fa# with time by considering size distribution of fine-grained olivine and Fe-Mg diffusion rates is in progress.

Keywords: CV3 carbonaceous chondrites

PPS021-10

Room:101

Time:May 23 11:15-11:30

Thermal metamorphism in type 3 Enstatite chondrites.

Mutsumi Komatsu^{1*}, Timothy Fagan¹, Takashi Mikouchi²

¹Earth Sciences, Waseda University, ²Earth and Planetary Sci., Univ. of Tokyo

Introduction:

Enstatite chondrites represent initial formation and metamorphism under highly reduced conditions. Like the other chondrite groups, the enstatite chondrites underwent various degrees of thermal metamorphism resulting in distinct petrologic types [1]. Type 3 chondrites are the least metamorphosed type among chondrite groups. For ordinary chondrites, Sears et al. [2] subdivided type 3 into ten finer divisions (type 3.0 through 3.9) using thermoluminescence (TL) sensitivity as an indicator of metamorphic grade. Subsequently, some mineralogical changes with increasing subtype have been identified [3]. An approach similar to that of [3] has been applied to enstatite chondrites [4]; however, a systematic understanding of metamorphic reactions has not been attained and metamorphic sub-types have not been established for enstatite chondrites. In this study, we examined 5 enstatite (EH3) chondrites in order to assess variations in texture and mineral compositions among the EH3 chondrites (ALHA81189, ALH84170, Sahara97096, Y-691, and PCA82518). We also compared these observations with EH4 (Indarch) and EH5 samples (St.Marks and LEW88180) to gain a broad perspective of metamorphism of EH chondrites.

Results and Discussion:

All of EH3 chondrites in this study are dominantly composed of FeO-poor pyroxene. Metallic and sulfide minerals occur as complex nodules which are composed of combinations of troilite, Fe-Ni metal, perryite, niningerite, djerfisherite, and daubreelite. Occasionally, oldhamite is also present.

ALHA81189 contains well-defined chondrules and chondrule fragments. Many chondrules are rimmed by silica or silica-rich rims in ALHA81189 and Y-691, whereas silica or silica-rich rims are not as abundant in ALH84170 and Sahara97096. In PCA82518, silica-rich rims were not identified. Instead, euhedral silica is observed inside chondrules.

Sulfide nodules are abundant in all EH3s. Sulfide/metal nodules in ALHA81189, ALH 84170 and Y-691 have sizes and shapes similar to silicate chondrules and are composed of combinations of troilite, kamacite, daubreelite, and niningerite. Generally, troilite and daubreelite occupy the cores of the spherules whereas kamacite usually occurs in the outer portions. Sulfides are more dispersed in PCA82518; the core-rim structure as described above is absent. In contrast, mixed sulfide/metal nodules are rare and sulfides tend to occur as dispersed crystals in Indarch (EH4), St. Marks (EH5) and LEW 88180 (EH5).

The Fa content of olivine, Fs content of pyroxene, and Ti and Cr contents in troilite show wide ranges of composition in the EH3 chondrites. Ti concentrations of troilite in ALHA81189 are lower than in the other EH3s, and those in PCA are the highest.

Based on the textural characteristics of EH3 chondrites, we can subdivide EH3s into 3 distinct groups: (1) Primitive, ALHA81189 and Y-691; (2) low degree of metamorphism, ALH84170 and Sahara 97096; moderately metamorphosed, PCA82518. This trend is supported by the chemical compositions of pyroxene and troilite; primitive EH3s have high Fs content in pyroxene and low Ti content in troilite, whereas metamorphosed EH3s have lower Fs content in pyroxene and higher Ti content in troilite. These results suggest that the reduction (lower $f(O_2)$) occurred during thermal metamorphism [5].

References: [1] Zhang et al. (1995) JGR, 100, E5, 9417-9438. [2] Sears et al. (1983) LPS XIV, 682-683. [3] Grossman J. N. and Brearley A. J. (2005) Meteoritics & Planet. Sci., 40, 87-122. [4] Bendersky et al. (2007) LPS, XXXVIII, 2077. [5] Fagan T. J. et al. (2010) LPS XXVII, 1534.

Keywords: meteorites, chondrites, metamorphism

PPS021-11

Room:101

Time:May 23 11:30-11:45

Mn-Cr dating of dolomite in the Ivuna CI chondrite

Wataru Fujiya^{1*}, Naoji Sugiura¹, Yuji Sano¹

¹The Univ. of Tokyo

CI chondrites are compositionally the most primitive rocks among the solar system materials, although they experienced pervasive aqueous alteration. In order to decipher their geological history, it is important to determine the timescale of the aqueous activity in the CI chondrite parent body.

⁵³Mn-⁵³Cr systematics (⁵³Mn decays to ⁵³Cr with a half-life of 3.7 Myr) of dolomite and breunnerite measured with ion probes have been reported for the Orgueil CI chondrite (e.g. Hoppe et al., 2007). For the Ivuna CI chondrite, there is only one report on dolomite. Hence, further investigations are needed for the accurate Mn-Cr age determinations. Here we report Mn-Cr systematics of six dolomite grains in Ivuna.

Six dolomite grains in Ivuna were analyzed for Mn-Cr systematics with the NanoSIMS installed at Atmosphere and Ocean Research Institute, the Univ. of Tokyo. Their Mn concentrations range from 0.7 to 2.7 wt.%. ⁵³Ca⁺, ^{52,53}Cr⁺ and ⁵⁵Mn⁺ were measured with the O⁻ primary ion beam (~5 micrometers in diameter, ~1 nA). The ⁵⁵Mn/⁵²Cr relative sensitivity factor (RSF) of 0.690 is determined using a synthetic calcite standard doped with Mn and Cr (Sugiura et al., 2010). Errors on ⁵³Cr/⁵²Cr and ⁵⁵Mn/⁵²Cr ratios are based on the counting errors. ⁵³Cr excesses of the Ivuna dolomite are represented as permil deviations from the ⁵³Cr/⁵²Cr ratio of the standard assumed to be 0.1134 (Lodders et al., 2009).

Obtained ⁵³Cr excesses are well correlated with ⁵⁵Mn/⁵²Cr, which indicates the in-situ decay of ⁵³Mn. All data lie on a single regression line in the isochron diagram (i.e., no difference is found among slopes of the six grains) and the slope of the best fit line for the whole data corresponds to (⁵³Mn/⁵⁵Mn)₀ of (2.64 +/- 0.44) x 10⁻⁶. Then an absolute age of 4562.5 +/- 0.8/-1.0 Ma is calculated for dolomite in Ivuna using the LEW86010 angrite as a time anchor (Amelin, 2008; Lugmair and Shukolyukov, 1998).

The present data for dolomite in Ivuna gives a younger age than that in Orgueil reported by Hoppe et al. (2007) and Petit et al. (2009). However, these studies used silicate standards for calibration of ⁵⁵Mn/⁵²Cr ratios of dolomite, which resulted in systematic errors in the obtained ages. If the RSFs are corrected, then the Mn-Cr ages of the Orgueil dolomite become consistent with that of the Ivuna dolomite. The Ivuna dolomite in this study is older than the Orgueil and Ivuna dolomite reported by Endress et al. (1996), which is unlikely due to the difference in the RSFs used. The reason for this discrepancy is unknown at this time.

Fujiya et al. (2011) reported Mn-Cr ages of calcite and dolomite in four CM chondrites, indicating that calcite and dolomite in CM and CI chondrites formed around the same time. Because calcite precipitation appears to have preceded dolomite formation (de Leuw et al., 2010), our data imply contemporaneous accretions of the CI and CM chondrite parent bodies and dolomitization occurred soon after calcite precipitation.

On the other hand, it seems that individual breunnerite grains in Orgueil show variable and younger ages than those of dolomite grains (Hoppe et al. 2007; Petit et al., 2009). Therefore, we conclude that the breunnerite formation persisted for at least 7 Myr following dolomite formation. Given that the Mn-Cr ages in Petit et al. are biased due to the RSFs, breunnerite formation (and therefore, aqueous alteration) in Orgueil lasted until ~4553 Myr (at least 10 Myr after dolomite formation in Ivuna).

Keywords: dolomite, CI chondrite, Mn-Cr dating, aqueous alteration

PPS021-12

Room:101

Time:May 23 11:45-12:00

Oxygen isotopic compositions of silicate grains associated with D-rich carbonaceous matters in a carbonaceous chondrite

Minako Hashiguchi^{1*}, Sachio Kobayashi², Hisayoshi Yurimoto¹

¹Natural History Sci., Hokkaido Univ., ²CRIS, Hokkaido Univ.

Organic matters enriched in D and/or ¹⁵N in chondrites are believed to have formed in cold molecular cloud and/or outer protoplanetary disk. The organic matters would be produced in ice coatings on interstellar dust grains in the cold interstellar cloud [e.g. 1].

In our previous study, we discovered D-rich carbonaceous matters in NWA 801 (CR2) carbonaceous chondrite using hydrogen isotope imaging, and classified their morphology [2]. Hydrogen isotopic compositions of these carbonaceous matters are 1360-11000 permil of delta-D. Some D-rich carbonaceous matters in the NWA 801 are ring shaped globules containing a silicate grain in the center (ring globule), and aggregates with silicate grains (globule aggregate).

In this study, we focus on the silicate grains associated with D-rich carbonaceous matters. Their oxygen isotope compositions were measured by isotope imaging using isotope microscope in Hokkaido University [3].

Oxygen isotopic compositions of the silicate grains analyzed here are not different from the isotopic composition of solar system. The results suggest that these silicate grains have formed in the solar system. Therefore, it is plausible that the ring globules and the globule aggregates were formed on the silicate grains in outer protoplanetary disk in the early solar system. However, it is difficult to reject a possibility that most presolar grains in the cold molecular cloud have similar oxygen isotopic compositions with materials formed in the solar system and the ring globules and globule aggregates have formed in the cold molecular cloud.

In the future work, we will measure the oxygen isotopic compositions of more numbers of ring globules or globule aggregates. The dataset will be helpful to reveal formation region of D-rich carbonaceous matters in meteorites.

References

- [1] Li, A. and Greenberg, J. M. (1997) *Astron. Astrophys.*, 323, 566
- [2] Hashiguchi, M. et al. (2010) 73rd Annual Meeting of the Meteoritical Society., 5181
- [3] Yurimoto, H. et al. (2003) *Appl. Surf. Sci.*, 203, 793

Keywords: Carbonaceous chondrite, Organic material, Oxygen isotopic composition, Isotopography

PPS021-13

Room:101

Time:May 23 12:00-12:15

New insight into origin and evolution of insoluble organic matter in meteorites

Yoko Kebukawa^{1*}, Ying Wang¹, George Cody¹

¹Carnegie Institution of Washington

Organic matter in meteorites provides us clues to understand the early Solar System history. Our recent study revealed that insoluble organic matter (IOM) in primitive chondritic meteorites is predominantly derived from the polymerization of interstellar formaldehyde with incorporation of ammonia, evidenced by molecular spectroscopic characters. Here we show molecular structures of laboratory synthesized formaldehyde polymer and compare with the formose solids to chondritic IOM using various spectroscopic methods; solid state ¹³C nuclear magnetic resonance (NMR), Fourier transform infrared (FTIR) spectroscopy and X-ray absorption near edge structure (XANES). We will discuss about the kinetics of polymer yield, and effects of silicate minerals coexisting with chondritic organic matter. Isotopic exchange experiments with formaldehyde polymer and water also can explain the origin of deuterium enrichment in the IOM from carbonaceous chondrites. We featured ¹H-²H cross polarization NMR which allows us to see site-specific deuterium enrichment in organic polymers. The results show that organic hydrogen is very exchangeable with water. The deuterium enrichment of chondritic IOM could be explained by the deuterium exchange with water during aqueous alteration.

The final molecular structure of chondritic IOM has been shown to reflect the extent of parent body processing, and to have significant variations among chondrite classes and groups. The principal inference has been that the molecular structure of IOM changes as a result of environmental conditions in the parent body. Our recent studies of individual lithology of the Tagish Lake meteorite provides insight into the wide range of molecular structure complexity that existed locally in a single parent body. We conducted heating experiments of most pristine IOM from Tagish Lake. The molecular structure evolution observed in Tagish Lake is representable with flash heating with several hundred degree C. Thus, the changes in Tagish Lake IOM from different lithologies may reflect differing degrees of flash heating due to impact processes.

Keywords: insoluble organic matter, chondrites, NMR, FTIR, XANES

PPS021-14

Room:101

Time:May 23 12:15-12:30

Three-dimensional observation of organic nanoglobules by microtomography and evaluation of CT images by image simulation

Tooru Matsumoto^{1*}, Akira Tsuchiyama¹, Keiko Nakamura-Messenger², Michael.E.Zolensky², Tsukasa Nakano³, Kentaro Uesugi⁴

¹Earth and Space Sci., Osaka Univ, ²NASA Johnson Space Center, ³GSJ/AIST, ⁴JASRI

Spherical organic matters called organic nanoglobules of a few hundred micrometers in typical size were found in carbonaceous chondrites, IDPs, and dust from comet 81P/Wild2 [1-3]. Most of them have hollow structures. It has been suggested that the organic nanoglobules were formed from organics-ice particles in the molecular cloud or the protoplanetary disk in the solar system [4]. Aqueous alteration of organic matters is also suggested as alternative possible formation processes [1]. If one of the hypotheses is true, hollow regions of the globules might be filled with H₂O-rich ices or fluids. However they have not been detected because they had been lost during destructive observations, such as transmission electron microscope (TEM) observation, in the previous studies.

In the present study, we tried to observe organic globules non-destructively using synchrotron radiation-based absorption-contrast imaging X-ray microtomography [5] in order to determine the existence of fluids in the hollows of nanoglobules. The imaging experiments were made at the beamline BL47XU of SPring8 with the photon energy of 7.0 keV. CT images were reconstructed from 1800 projections and successional CT images of about 800 slices were obtained for the 3-D structure of Tagish Lake meteorite. The voxel size in the CT images is 40.8 nm³. Then, we microtomed some samples and observed ultra-thin sections under a TEM. Comparison between the CT and the TEM images showed that nanoglobules can be observed in the CT images. But CT images of nanoglobules are affected by X-ray refraction. So we could not determine materials in nanoglobules from CT images alone. There are many spherical objects as candidates of organic nanoglobules in the CT images.

In order to identify nanoglobules and to determine whether or not any fluids are present in the hollows, we tried to evaluate CT images by simulating CT images by considering X-ray absorption and refraction for nanoglobules with hollow or water, which are surrounded by saponite, a main constituent mineral of Tagish Lake meteorite matrixes. We calculated transmittance of X-rays that pass the sample with absorption and refraction and reach a detector. Actual tomography experiments were performed under an imaging system with a Fresnel zone plate (FZP). The location of the detector in the simulation corresponds to a focal spot of the FZP. Simulated CT images were made by reconstruction with the pixel sizes of the detector (40.8 nm) and measured point spread function (FWHM = 360 nm). Simulated CT images indicated that nanoglobules containing water cannot be distinguished from those without hollow in CT images. When organic rims are thin, CT images of nanoglobules with hollow cannot not be distinguished from those of simple spherical pores. The effective spatial resolution of nanoglobules is about 300 nm. Comparison between CT images of nanoglobules identified by the TEM observation and simulated CT images suggested that this nanoglobules might not contain any water.

The simulation also revealed that three-dimensional shape of nanoglobule can be estimated by CT images. Three-dimensional distribution of nanoglobules can be also obtained by CT images. We can grind the sample to the position right above a nanoglobule detected by tomography and analyze a fluid in the nanoglobule using a microanalysis, such as nano SIMS, if fluid is reserved.

[1] Nakamura K. et al (2002) *Int. J. Astrobiol.*, 1, 179. [2] Messenger S. et al. (2008) *LPS XXXIX*, Abstract #2391. [3] De Gregorio B. T. (2009) *LPS XXXX*, Abstract #1130. [4] Nakamura-Messenger K. et al (2006) *Science*, 314 1439-1442. [5] Uesugi K et al (2006) *Proceedings of SPIE6318:63181F*.

Keywords: X-ray microtomography, organic nanoglobule, carbonaceous chondrite, image simulation

PPS021-P01

Room:Convention Hall

Time:May 23 16:15-18:45

Trace element imaging and semi-quantitative analysis of meteorites by Laser ablation ICP-MS

Souichiro Fukushima^{1*}, Izumi Nakai¹, Masahiro Oishi²

¹Tokyo University of Science, ²TDK

Introduction

So far, electron microprobe has been used to study two dimensional distributions of elements in earth and planetary samples. However, the sensitivity of the method is insufficient for trace elements analysis. Furthermore, though synchrotron radiation X-ray fluorescence imaging has high sensitivity, micro-XRF imaging of trace heavy elements is still difficult to perform. In this study, LA-ICP-MS method was adopted to analyze two dimensional distributions of trace heavy elements in meteorites. This method is highly sensitive and is suitable for the analysis of meteorites, because it allows the analysis of two dimensional distribution of trace elements up to 72 elements. In this study, LA-ICP-MS was applied to obtain semi quantitative information of the trace elements and to reveal correlation of the elemental distribution in the sample.

Experiment

Analyzed samples were stony meteorite (NWA2086), iron meteorites (Sikhote-Alin, Gibeon, Odessa, Henbury, Nantan) and stony-iron meteorite (Fukang Pallasite). The LA instrument used in this study was a UP-213 Universal Platform (New Wave Research, USA), coupled to an Agilent 7500s ICP-MS instrument (Agilent Technologies, USA). Semi-quantitative analysis was performed based on the external standard glass sample NIST 612. The imaging was obtained by combination of the line scans on fixed area.

Results and Discussion

Our LA-ICP-MS imaging of the stony meteorite successfully revealed the distribution of the platinum Group elements (Os, Ir, Pt), rare earth elements (La, Ce, Sm, Eu) and other heavy elements accumulated in CAI (Calcium-Aluminium rich Inclusion). A correlation of siderophile elements (Ni, Co and also) are observed in a matrix part of the meteorite. On the other hand, in iron meteorites and stony-iron meteorite, a local correlations of elements in Fe-rich regions was observed though uniform distributions were observed for other elements. Semi-quantitative analysis of rare earth elements were successfully carried out and revealed a distribution pattern of the rare-earth elements in the sample, demonstrating a potential ability of quantitative two dimensional imaging of trace elements in the samples. In conclusion, the LA-ICP-MS imaging can provide elemental distribution of light and heavy elements in ppm level, which could not be obtained by using any other analytical methods. We believe that the LA-ICP-MS imaging will become a powerful analytical tool in earth and planetary sciences.

Keywords: ICP-MS, imaging, semi-quantitative analysis

PPS021-P02

Room:Convention Hall

Time:May 23 16:15-18:45

Carbon-XANES spectroscopic comparison of Q-gas rich and depleted fractions from Allende meteorite

Hikaru Yabuta^{1*}, Sachiko Amari², Jun-ichi Matsuda¹, Toshiaki Hasegawa³, David Kilcoyne⁴

¹Osaka Univ., Dept. Earth and Space Sci., ²Washington Univ. Lab. Space Sci., ³Osaka University, UHVEM, ⁴Advanced Light Source, LBNL

Introduction:

Although the planetary noble gases enriched in the heavy noble gases, Q gases, have been frequently studied, phase Q itself is yet to be identified. Matsuda et al. (2010) has reported that TEM observations did not show clear difference between Q-rich- and depleted- carbonaceous materials, while the Raman spectroscopic differences were observed between the two. They concluded that release of Q gases is not accompanied by mass loss but resulted from rearrangement of carbon structure during removal of Q (oxidation). Our previous study has revealed that the physically separated Q-rich density fraction may be rich in diamond-related sp^3 carbon. Thus, the release of Q gases and/or phase Q could be related to carbon functional group chemistry rather than carbonaceous morphology. This study focuses on the XANES analyses of Q-rich- and depleted- materials from Allende meteorite to refine carbon chemistry that is likely associated to the release of Q gases. Moreover, Q-rich fractions obtained via the suspension and physical separation from Allende, respectively, are analyzed for comparison.

Experimental:

An Allende meteorite was treated with HF-HCl for preparing an acid resistant carbonaceous residue. During the removal of elemental S from the residue with CS₂, One-seventh of the total fraction of the residue suspended in the supernatant was recovered (AMD3). The rest of the fraction (AMD1), which is rich in Q gases, was further treated with Na₂Cr₂O₇ to remove Q gases, yielding the oxidized residue, AMD2. Apart from AMD samples, a Q-rich floating fraction (G1), was obtained by the freeze-thaw disaggregation of Allende meteorite in stainless beaker. All the samples were embedded in sulfur and ultramicrotomed. Carbon-XANES of these samples was conducted using STXM at Beam line 5.3.2, at the Advanced Light Source, Lawrence Berkeley National Laboratory.

Results and discussion:

In C-XANES spectra of AMD1 and 2, aromatic and aliphatic carbons are much lower in AMD2 than those in AMD1. Carbonyl carbon is slightly higher in AMD2 than that in AMD1. On the other hand, the peak intensities of 1s- σ^* exciton derived from graphene, are not changed between AMD1 and 2. The differences in molecular features between AMD1 and 2 may not be directly reflected by phase Q, but more likely indicate the changes in major organic macromolecule by oxidation. Nonetheless, the depletion of aliphatic and production of carbonyls probably influence the structural rearrangement related with the release of Q-gases. No quantitative change of 1s- σ^* exciton intensity before and after oxidation indicates that phase Q is unlikely related to graphene.

Only one clear difference between C-XANES spectra of AMD1 and 3 is a peak at 287.43 eV in AMD 3 is remarkably developed compared to AMD1. A peak around at this energy is generally assigned to aliphatic carbon, or alternatively, another sp^3 carbon such as -C-CF of fluorinated diamond (Yu et al. 2003). The peak may have an important relation to Q-richness, since noble gas concentrations in AMD3 are 2-4 times higher than those of AMD1 (Amari et al. 2003).

G1 showed a quite different C-XANES spectrum from those of AMD1 and 3. While aromatic carbon is low, two unidentified peaks are detected. One of the two peaks is possibly derived from diamonds or their related compounds. Such spectral features are very similar to those in the Q-rich density fraction. Additionally, C-XANES spectra of different regions of G1 are heterogeneous. These spectra are not exactly the same as those of individual density fractions in our previous study. It may be because the individual density fractions show more detailed spectral features that were covered in bulk fractions, or might have been partially contaminated with Teflon beaker used in the past treatment by Matsuda et al. (1999). To summarize, it is further suggested that some sp^3 carbon may be related to the release of Q gases and/or phase Q.

Keywords: meteorite, chondrite, Q, carbonaceous matter, XANES, noble gas

PPS021-P03

Room:Convention Hall

Time:May 23 16:15-18:45

Infrared and raman spectroscopic analyses of the chondritic organic matter shot into silica aerogel by impact experiment

Yuichiro Ogata^{1*}, Hikaru Yabuta¹, Satoru Nakashima¹, Kyoko Okudaira², Taro Moriwaki³, Yuka Ikemoto³, Sunao Hasegawa⁴, Shinichi Yokobori⁵, Hajime Mita⁶, Kensei Kobayashi⁷, Eiichi Imai⁸, Hirofumi Hashimoto⁴, Makoto Tabata⁴, Yuko Kawaguchi⁵, Tomohiro Sugino⁵, Hajime Yano⁴, Masamichi Yamashita⁴, Akihiko Yamagishi⁵, TANPOPO Working Group⁴

¹Osaka University, ²University of Aizu, ³JASRI/SPring-8, ⁴ISAS/JAXA, ⁵Tokyo University of Pharmacy, ⁶Fukuoka Institute of Technology, ⁷Yokohama National University, ⁸Nagaoka University of Technology

Introduction:It has been suggested that sources of the prebiotic organic molecules were delivered to the early earth by meteorites, comets, and cosmic dusts (Exogenous delivery) (Chyba and Sagan, 1992). It is important to unravel the compositions and structures of organic matter in the small primitive bodies for better understanding the origin and chemical evolution of the prebiotic molecules in space. Although indigenous organic matter in meteorites and cosmic dusts has been known to be well preserved, some could be heated and lost during atmospheric entry or exposed to contamination from terrestrial materials. In order to collect the astromaterials without these problems, the cosmic dust collection with ultralow-density silica aerogel placed on International Space Station is planned (TANPOPO mission). However, the possible alteration of organic matter by impact heating upon aerogel capture is an unsolved issue. In this study, the high velocity impact experiment of meteorite powders was conducted for the purpose to evaluate the possible alteration of organic molecular compositions of meteorites before and after the impact.

Experimental:One hundred micron-sized Murchison meteorite powders were shot into silica aerogel by the impact velocity of 4km/s, using the two-stage light gas gun at Space Plasma Laboratory, ISAS, JAXA. The meteorite particles penetrated into the aerogel were carefully picked up by tungsten needle and fine brush, sandwiched with two Al plates, and hand-pressed. For comparison, non-shot Murchison meteorite powders were prepared on the Al plates as well. These shot- and non-shot- Murchison samples were analyzed by micro-FTIR (JASCO, FTIR-620) and micro-Raman spectrometers, respectively. In addition, infra-red imaging of the shot Murchison particles was conducted by the high brilliance micro-FTIR (Bruker, IFS120HR), BL43IR, Spring-8. Step size is 10 micro metre, mode of measurement is reflection, wavenumber resolution is 4cm^{-1} .

Results and discussion:In the micro-FTIR spectra of the three shot Murchison particles, the peaks assigned to aliphatic carbon ($3000, 2900, 2880\text{cm}^{-1}$), aromatic carbon (1600cm^{-1}), and SiO (1100cm^{-1}) were identified. The infra-red imaging detected the local regions where aliphatic and aromatic carbons and SiO are abundant, respectively, from the particles. The distributions of aliphatic and aromatic carbons were very similar, but not completely overlapped. One of the two SiO-rich regions was almost consistent with the organic-rich region while another was not. In general, aliphatic carbon in carbonaceous chondrites has been known to be depleted by heating (Yabuta et al.2005). Detection of aliphatic carbon from the shot Murchison particles in this study implies that organic matter in the particles is not highly altered by the impact velocity of 4km/s.

In the Raman spectra of the three shot Murchison particles, from which organics were identified by micro-FTIR, D- ($\sim 1350\text{cm}^{-1}$) and G- ($\sim 1580\text{cm}^{-1}$) bands were detected. The peak positions and widths of D- and G-bands for the shot Murchison particles were similar to those for the non-shot- Murchison particles. Thus, again, it is unlikely that organic matter in Murchison particles is altered by the impact experiment. The G-band positions and widths for the shot Murchison particles were similar to those for insoluble organic matter from Murchison meteorite (Busemann et al. 2007). However, their D-band positions and widths were different, which is probably due to the difference of analytical conditions. Organics were not detected from the other four particles by infrared nor Raman. This may be because the volatile components in meteorites were partially vaporized or moved due to the impact heating. Further investigation will be necessary to improve the feasibility of the cosmic dust analyses s collected in TANPOPO mission.

Keywords: meteorite, cosmic dust, impact heating, infrared spectroscopy, Raman spectroscopy, TANPOPO mission

PPS021-P04

Room:Convention Hall

Time:May 23 16:15-18:45

U-Pb Dating and D/H Ratio of Phosphates in the Martian Meteorite ALH84001.

Yoshihiro Ota^{1*}, Naoto Takahata², Yuji Sano², naoji sugiura¹

¹School of Science, University of Tokyo, ²AORI, University of Tokyo

The presence of water on Mars has been revealed by observations using spacecrafts, and elemental and isotopic analyses of Martian meteorites. In previous SIMS analyses of hydrogen, phosphate minerals containing OH group, for example an apatite($\text{Ca}_5(\text{PO}_4)_3[\text{OH}, \text{F}, \text{Cl}]$) and a whitlockite($\text{Ca}_9[\text{Mg}, \text{Fe}^{2+}](\text{PO}_4)_6\text{PO}_3\text{OH}$) were used. There are many studies that measured D/H ratios from the OH group in phosphates [1], [2]. Phosphate minerals are enriched in Uranium and U-Pb dating has been made in many studies [3]. We have measured U-Pb ages, D/H ratios and amounts of water of phosphates in the Martian meteorite, ALH84001 with a NanoSIMS. The goal of this study is to observe a secular variation of D/H ratios by Martian meteorites. Phosphate minerals in a thin section were detected by SEM-EDS and it was coated with gold films before the NanoSIMS measurement. For U-Pb dating by SIMS, primary O^- ions with a beam intensity of 10nA were used. Several points were measured in single grains of a phosphate mineral in a spot diameter of about 10 micrometer. The apatite produced from Prairie Lake called PRAP whose age was known [4] was used as a standard. This phosphate mineral crystallized about 4 billion years ago according to the U-Pb, Pb-Pb system. The age obtained in this study was consistent with those of the previous studies [3] within the experimental error. For D/H ratio measurements, primary O^- ions with a beam intensity of 1 nA were used. The spot size was about 3 micrometer. D/H ratios in a number of phosphate grains were measured. Surface water contamination could be negligibly small after the baking of the sample over night at 80 deg C under a high vacuum about 10^{-7} torr. The standard apatite for water measurement was driven from Morocco and some other places. The water of the Morocco apatite was extracted by heating at 1200 deg C for an hour in a vacuum line, and the abundance was measured by a manometric method. Observed D/H ratios of ALH 84001 tended to show a mixing line between the martian heavy hydrogen and terrestrial light hydrogen. Even though it is difficult to estimate the martian end-members, the data distribution suggests that the D/H ratio is at least higher than 3000 permil. The amount of water was found to be very small. This result shows a little heavier than previous results [5]. In previous studies, U-Pb age was obtained by spot analysis of several phosphate minerals. In this study it is possible to determine the age of an individual phosphate grain with several spots. We have measured the D/H ratio of the same grain. The data reflect the water on Mars at 4.0 Ga. At the poster session I will discuss the meaning of the U-Pb age and the D/H ratio.

[1] Leshin L. A. et al.(2000) *Geophys Res. Lett.* **27** 2017-2020, [2] Greenwood J. P. et al.(2008) *Geophys Res. Lett.* **35** L05203, [3] Terada K. et al.(2003) *Meteoritics&Planet.Sci.* **38** 1697-1703, [4] Sano Y. et al.(1999) *Chem. Geol.* **153**, 171-179, [5] Sugiura N. and Hoshino M. (2000) *Meteorol. Planet. Sci* **35**, 373-380.

Keywords: martian meteorite, alh84001, U-Pb dating, D/H ratio, phosphate

Mineralogical characterization and formation process of shock-induced melt veins in the Efremovka CV3 chondrite

Chisato Sekigawa¹, Yusuke Seto^{1*}, Akira Miyake², Kazushige Tomeoka¹

¹Dept. Earth and Planet. Sci., Kobe Univ., ²Dpt. Geology and Mineral., Kyoto Univ.

An understanding of shock effects is important to bring out the impact history of the solar system. A shock-induced melt vein is one of the typical textures caused by impact; the vein is considered to be formed by rapid shear melting and be solidified along the shearing plane in extremely short times. Mineralogy of the shock-induced melt veins have been well studied in highly shocked ordinary chondrites so far, while there are few studies of carbonaceous chondrites which are usually considered to have been experienced relatively weak shock metamorphism.

Efremovka, grouped as a CV3 carbonaceous chondrite, is known to be experienced a strong shock metamorphism classified with a shock stage of S4. Although the previous studies on Efremovka mainly focused on the chemical/isotopic properties, the detailed mineralogical and petrographic characteristics remain to be known. We made a SEM observation of the Efremovka thin sections with a total area of about 200 mm², and found distinguish veins or puddles including spherical globules of Fe-Ni metal, Fe-sulfide in the matrix. In order to clear whether these objects have been actually experienced melting or not, and to clear its formation process, we undertook a mineralogical study regarding on the veins (tentatively called "melt vein") compared with the other area of the matrix (called "normal matrix") using transmission electron microscopy (TEM) and synchrotron radiation X-ray diffraction (SR-XRD).

The veins are often observed near chondrule-matrix boundaries, and sometimes penetrate into the adjacent chondrules or matrices. For site-specific samplings, the melt veins and the normal matrix were lifted up from the thin section and were trimmed to feasible shapes for SR-XRD and TEM experiments using a focused ion beam (FIB) technique. The SR-XRD and TEM experiments show the clear differences between the melt veins and the normal matrix, especially as to the constituent olivines. The unit cell volume data from SR-XRD and the TEM-EDX analyses consistently indicate that the olivine of the melt veins (Fo₇₃) is poorer in Fe contents than that of the normal matrix (Fo₄₅). A clear difference is also seen in the grain size; the olivine size in the melt veins is significantly larger (~300 nm) than that in normal matrix (~100 nm). Moreover, appearances of lattice defects in the olivines is different; from TEM observation, dislocation densities in the melt vein's olivines are much lower than those in normal matrix in spite of the evidence of the heavy shock impact.

These results indicate that the melt veins have certainly experienced a different formation process from that of normal matrix, which are apparently affected by melting and quenching processes. During these processes, olivine in the veins grew larger in size and become poorer in Fe contents than those in original matrix. On the other hand, as for most parts of Efremovka matrix escaping from melting, the shock wave effect can be found in compaction of matrix and high dense dislocations in the constituent minerals. The present study reveals that chemical and mineralogical disproportions are caused by melting and quenching process. Such shock-induced process may be one of the factors generating a diversity of meteorites.

Keywords: carbonaceous chondrite, melt vein, shock metamorphism, Efremovka, TEM, SR-XRD

Heterogeneity of chemical and mineral compositions of Bensour meteorite (LL6) in relation to Hayabusa sample analysis.

Takashi Nagano^{1*}, Tsuchiyama Akira¹, Shimobayashi Norimasa², Yuusuke Seto³, Yuuta Imai¹, Ryo Noguchi¹, Tooru Matsumoto¹, Matsuno Junya¹

¹Earth and Space Sci.,Osaka Univ., ²Earth and Planetary Sci., Kyoto Univ., ³Earth and Planetary Sci.,Kobe Univ.

The Hayabusa spacecraft returned to the earth last June. "Hayabusa" succeeded in observation of the asteroid Itokawa, and samples on the surface of Itokawa were recovered. Asteroids are considered to have information when they were formed in the early stage of the solar system, and it is expected that the clue to the information can be obtained by analyzing their samples. However, the maximum size of the sample particles recovered by "Hayabusa" is the order of 100 micro meters, and most of them are smaller than ten micro meters [1]. The chemical composition and mineral composition obtained from these small particles doesn't represent the material on the Itokawa surface. Then, it is necessary to examine how the chemical composition and the mineral composition change compared with the bulk when the sample becomes smaller in connection to the texture of meteorites.

It is proposed that the surface material of Itokawa is similar to LL5 or LL6 ordinary chondrite based on the infrared spectroscopic observation by "Hayabusa" [2]. In this study, heterogeneity of the chemical and mineral compositions was quantitatively examined by obtaining elemental mapping of the Bensour meteorite (LL6 chondrite). 13 elements (Al, Ca, Cr, Fe, K, Mg, Mn, Na, Ni, P, S, Si, Ti) were measured for two areas of about 4mmx4mm in a polished thin section, and elemental maps (images of 1024x1024 pixels) were obtained. In addition, mineral maps were made from the obtained elemental maps. The minerals contained in those ranges were olivine, Ca-poor pyroxene, Ca-rich pyroxene, plagioclase, apatite, whitlockite, taenite, kamacite, and chromite.

The elemental and mineral maps were divided into smaller areas by four, sixteen, and so on in the images. The standard deviations of the characteristic X-ray intensities of the elements and of the mineral modes were calculated as a function of the number of the division. The characteristic X-ray intensities and the mineral modes and changes of their standard deviations by increasing the number of the division were not greatly different among the two measured areas. This indicates that these areas roughly represent an average feature of this meteorite. The standard deviation of the characteristic X-ray intensity normalized its intensity increases with increasing the number of the division. The normalized standard deviations at the same number of the division for elements of low abundances, such as P, Ni and Cr, are larger than those of elements with high abundances, such as Si and Mg. This is due to the concentration of the elements with low abundances in specific accessory minerals, such as Ca phosphates, taenite, chromite for P, Ni and Cr, respectively, which are distributed locally. On the other hand, there is a different group of elements with low abundances, such as K, Mn and Ti. These normalized standard deviations are relatively small. These elements are included as minor elements in major minerals, such as plagioclase of K and pyroxenes for Mn and Ti. Based on the present study, if the Hayabusa sample is an LL6 chondrite, we can quantitatively expect deviations of the element and mineral compositions obtained from limited size of the sample by preliminary examination.

We are grateful to Dr. T. Fagan of Waseda University for providing the polished thin section of the Bensour meteorite.

[1] Nakamura T. et al. (2011) abstract in 42nd LPSC. [2] Abe M. et al. Science, 312, 1334-1338. [3] Tsuchiyama A. et al. (2011) abstract in this conference.

Keywords: Hayabusa, chondrite meteorite, composition

Conditions of aqueous alteration of C-type asteroids estimated from oxygen isotope ratios of carbonate in CM chondrites

Katsuki Yoshioka^{1*}, Tomoki Nakamura¹, Hirokazu Fuzimaki¹, Yuki kakazu¹

¹Department of Earth and Planetary Science

CM chondrites have undergone prevailed aqueous alteration that changed mineralogical and isotope signatures of water-bearing C-type asteroids (Zolensky and McSween, 1998; Clayton and Mayeda 1984). In the present study, we studied a CM chondrite GRA06172 that has never been studied in detail in order to estimate the degree and the conditions of aqueous alteration occurred on a meteorite parent body. A polished section was observed by a SEM/EDS and analyzed by an EPMA/ WDS. A small piece (200 microns in size) of matrix was analyzed by synchrotron radiation X-ray diffraction to identify minerals, since matrix minerals are too small to identify by using a scanning electron microscope.

SEM observations suggest that approximately half of the meteorite consists of primary rocks (Metzler et al., 1992) where chondrules were mantled by thick fine-grained rims and aggregates of PCPs occur on the rims. The other half is clastic matrix that was produced by fragmentation of the primary rock. This observation indicates that the meteorite is a breccia. Mesostasis glasses in both type-I and ?II chondrules are aqueously altered but most of anhydrous silicates such as olivine and low- and high-Ca pyroxenes are unaltered.

The results of the X-ray diffraction analysis indicate that matrix is composed mainly of serpentine and tochilinite, which suggests that matrix has undergone aqueous alteration. The presence of tochilinite limits the temperature experienced by this meteorite to be lower than 245C. (Gooding and Zolensky, 1992). In addition, sharp diffraction peaks from low-Ca pyroxene were detected. This indicates that some of anhydrous silicates survived aqueous alteration.

The EPMA analysis suggests that most of matrix composition fall within the area enclosed by composition PCP and two serpentine compositions on a Si-Mg-Fe ternary diagram as was reported in the McSween (1986). The average matrix composition changes with progressive alteration (McSween, 1986) and suggests that the degree of aqueous alteration experienced by GRA06172 is similar to or even higher than that for Murchison.

In addition, the mineralogical alteration index defined by Browning (1995) (when the number of oxygen of serpentine is nine, the index is calculated by $2 - (\text{Fe}3 + / (2 - \text{Si}))$) is approximately 0.65, which indicates that the meteorite altered to a degree higher than Murchison (1.57). Based on the CM chondrite classification scheme (CM2.6-2.0) defined by Rubin (2007), the average value of FeO/SiO₂ in PCP (2.8) and mineralogical and other characteristics of the meteorite suggest that it is classified to CM2.5 that is the same as Murchison. These results suggest that the extent aqueous alteration on GRA06172 is intermediate similar to or slightly higher Murchison, although small gaps are present between estimations from different models (i. e., McSween, 1986 vs Rubin, 2007).

There are many carbonate with sizes up to 100 microns in the matrix. Oxygen isotope analysis of the carbonate and co-existing serpentine is in progress using SIMS at Tohoku University (CAMECA ims-6F) so as to estimate water temperature and water / rock ratio during aqueous alteration.

Keywords: carbonatious chondrite, aqueous alteration, oxygen isotope

PPS021-P08

Room:Convention Hall

Time:May 23 16:15-18:45

Al-Mg isotope distribution in Type B CAI: partial melting and chronology

Shoichi Itoh^{1*}, Steven Simon², Lawrence Grossman², Hisayoshi Yurimoto¹

¹Natural History Sci., Hokudai, ²Dept. Geophys. Sci., The Univ. Chicago

Introduction: Oxygen isotopic compositions are heterogeneously distributed within and between minerals in coarse-grained CAIs, suggesting crystallization from different generations of melt. These minerals often plot on a straight line or multiple lines on an Al-Mg isochron diagram. From petrographic and O isotopic study, these CAIs have experienced at least two partial melting events (e.g., Simon et al., 2005; Itoh et al., 2009). In the present study, we report preliminary results of Al-Mg isotopic measurements of spinel and melilite in Golfball and TS34 to estimate the reset for Al-Mg isotope system of the multiple melting events of each melt.

Results and discussion: Al-Mg isotope analyses were performed with a Cameca ims-1270 SIMS instrument at Hokkaido University. These analytical procedures are described in detail elsewhere.

Two isochrons are defined by the Al-Mg data for these CAIs. For Golfball, the gehlenitic core melilite and rim melilite yield different initial $^{26}\text{Al}/^{27}\text{Al}$ ratios of 4.9 (8) and 1.9 (12) $\times 10^{-5}$, respectively. The age difference between the two isochrons is calculated to be about 1 My. For TS34, the spinel (through the origin) and the mantle melilite yield different initial $^{26}\text{Al}/^{27}\text{Al}$ ratios of 5.5 (4) and 4.5 (6) $\times 10^{-5}$, respectively. The age difference between the two isochrons is calculated to be about 0.2 My. These results are consistent with the multiple crystallization history by the results of petrographic study.

Keywords: SIMS, Al-Mg isotope, CAI, oxygen

PPS021-P09

Room:Convention Hall

Time:May 23 16:15-18:45

Noise analysis of SCAPS-II ion imager

Naoya Sakamoto^{1*}, Satoshi Aoyama², Shoji Kawahito³, Hisayoshi Yurimoto⁴

¹CRIS, Hokudai, ²Brookman Technology Inc., ³Electronics, Shizuoka Univ., ⁴Natural History Sci., Hokudai

A solid-state ion imager SCAPS has been proposed and demonstrated two-dimensional isotope ratio imaging with permil precision coupled with a stigmatic SIMS. The SCAPS system can measure high ion flux with an accuracy of the statistical error. However, the readout speed currently optimized at 0.05 frames/s is not sufficient for the time-critical applications. In order to realize real-time readout without loss of quantitative capability, high sensitivity is needed to overcome the read noise. The output signal fluctuation from SCAPS caused by 1 incident ion (i.e., conversion gain) was 30 micro V/ion pixel, whereas the read noise was 85 micro V. We evaluated newly designed ion imager SCAPS-II with higher conversion gain and noise reduction mechanism to achieve high-sensitivity corresponding to real-time readout.

The SCAPS-II has 504x504 pixel 7 x 7 micron in size with 65% fill factor. Improvement of the conversion gain can be achieved to reduce the pixel capacitance according to the relationship of $Q = CV$ where Q is the accumulated charge, C is the capacitance, V is the output voltage. The pixel capacitance of SCAPS-II is designed to 3.5fF, which is 4 times smaller than SCAPS (14fF). In order to increase dynamic range on the image detection, the conditional reset function was incorporated.

We also incorporated noise-reducing mechanism by multiple signal sampling using a switched capacitor (SC) integrator. The analog signal of pixel is sampled for multiple times as a difference voltage between pixel signal and a reference voltage via capacitor. The voltage is integrated in analog memory consisting of an amplifier with a feedback capacitor. The multiple sampling circuits are installed into each column totally 504 units and sample the signal of pixels in a row containing 504 pixels selected by a row selection pulse at the same time. This function realizes 16 times sampling for one pixel signal at 10 frames/s and 12.5 frames/s with 1 time sampling. The 2-line analog buffer output the integrated signal to read faster twice.

The conversion gain for ion was evaluated using a SIMS instruments (Cameca ims-1270). The imager is installed in a vacuum chamber and cooled at 173K to achieve long integration time by reducing thermally generated dark current. In order to decrease the noises including fixed pattern noise, nondestructive readout correlated double sampling is used to subtract a dark frame from a signal frame obtained without pixel reset. The incident ion number is counted by Faraday cup attached to the SIMS instrument. The saturation level of signal is about 5×10^3 ions/pixel. The noise is increasing statistically until the noise floor becomes dominant. The conversion gain of SCAPS-II was estimated to be 150 micro V/ion, which is 5 times larger than SCAPS. The noise using multiple-sampling method is not decrease along the slope-1/2 line. In order to investigate the noise source, the different sampling sequence called frame-averaging method is applied. The frame averaging sequence samples the pixels signal once every frame rates and averaging the frames while the multiple-sampling method samples multiple times in tens of micro sec order. The frame-averaging method takes long time for sampling but the noise reduction efficiency is higher than multiple-sampling method under 50 micro V. However the noise source is not clarified yet, the possible noise source is the 1/f noise of the MOS transistor because the difference between multiple-sampling method and frame-averaging method is the required time in sampling.

The capability of single ion detection is evaluated with the combination of multiple-sampling method and frame-averaging method. The frame ratio is 3.5 frames/s, therefore, it takes 14.4 seconds to obtain the ion image. The histogram of imager output of ion incident region shows the peak around 150 micro V. Considering the conversion gain of 150 micro V/ion, this peak indicates single ion signal.

PPS021-P10

Room:Convention Hall

Time:May 23 16:15-18:45

Hydrothermal alteration experiments of amorphous silicates: effect of organic-inorganic interaction.

Ryo Noguchi^{1*}, Akira Tsuchiyama¹, Hikaru Yabuta¹, Satoshi Ichikawa²

¹Earth and Space Sci., Osaka University, ²Nanoscience Design, Osaka University

Most of carbonaceous chondrites with primitive chemical compositions have experienced aqueous alteration in their parent bodies. In order to understand the formation of minerals during the aqueous alteration process, we have previously carried out hydrothermal alteration experiments using Fe-free amorphous silicates with CI chondritic composition [1]. That study showed that saponite, serpentine, calcite and a relatively small amount of aragonite are formed from amorphous silicates and de-ionized water. This study focuses on the organic-inorganic interaction upon aqueous alteration of chondrites, since carbonaceous chondrite contains large amounts of organic compounds (~2%) [2] that could have been involved to formation of some minerals, such as carbonates.

The glass of the system, $\text{SiO}_2\text{-MgO-Al}_2\text{O}_3\text{-CaO-Na}_2\text{O}$, with the CI chondrite chemical composition was used. Three major elements, Fe, Ni and S, were excluded from the system for simplicity to avoid the change of the redox states. The glass sample was ground to make micron-scale powders. Two kinds of amino acids, glycine and alanine, were used as the analogue of whole organic matter in the carbonaceous chondrites. The ratio of alanine to glycine is 2.56:1.00, based on that in the GRA95229 which is weakly altered CR chondrite [3]. Silicates (100 mg), amino acids (23 mg) and de-ionized water (0.1 or 0.5 ml) were placed in Teflon vessels so that water to rock mass ratios were 1.0 and 5.0, sealed with stainless jacket, and were heated in an electric furnace at 150°C for 1, 2, 4 and 8 weeks under water saturated vapor pressures (approximately 3.0 bars). After heating experiments, vessels were rapidly cooled to room temperature in water. Solid products were recovered from solutions and dried in vacuum at room temperature. Parts (~80 mg) of solid materials were extracted with hot Milli-Q water for 24 hrs. The water extracts were analyzed with high-performance liquid chromatography (HPLC) to quantify the concentrations of amino acids. Solid products were analyzed with powder X-ray diffractometer (XRD).

In the XRD patterns of all the samples obtained from the hydrothermal experiments with different heating times, two major phyllosilicates, serpentine and saponite were identified. Aragonite, minor phase in CM chondrite, was also formed in all the experiments. However, calcite was not formed. The concentrations of alanine and glycine decreased with increasing time of heating, which is consistent with the trend of amino acid concentrations in aqueous-altered carbonaceous chondrites. On the other hand, the ratio of alanine to glycine decreased with increasing time of heating. This is a reverse trend to that of carbonaceous chondrites.

[1] Noguchi et al. (2011) 42th LPSC, abstract #1789

[2] Pizzarello et al. (2006) Meteorites and the Early Solar System II. 625-651

[3] Martians et al. (2007) Meteoritics and Planetary Science 42, 2125-2136

Keywords: carbonaceous chondrites, aqueous alteration process